Published in final edited form as:
Eur J Cell Biol. 2003 May ; 82(5): 209–221.

Loss of function and impaired degradation of a cataract-associated mutant connexin50

Viviana M. Berthoud[1),a], **Peter J. Minogue**[a], **Jun Guo**[a], **Edward K. Williamson**[b], **Xiaorong Xu**[c], **Lisa Ebihara**[c], and **Eric C. Beyer**[a]

[a]Department of Pediatrics, Section of Hematology/Oncology, University of Chicago, Chicago, IL/USA

[b]Department of Molecular Genetics and Cell Biology, University of Chicago, Chicago, IL/USA

[c]Department of Physiology and Biophysics, Finch University of Health Sciences, North Chicago, IL/USA

Abstract

A mutant human connexin50 (hCx50), hCx50P88S, has been linked to cataracts inherited as an autosomal dominant trait. The functional, biochemical and cellular behavior of wild-type and mutant hCx50 were examined in transfected cells. hCx50P88S was unable to induce gap junctional currents by itself, and it abolished gap junctional currents when co-expressed with wild-type (wt) hCx50. Cells transfected with hCx50P88S showed cytoplasmic accumulations of Cx50 immunoreactivity in addition to staining at appositional membranes; these accumulations did not significantly co-localize with markers for the endoplasmic reticulum, Golgi apparatus, lysosomes, endosomes or vimentin filaments. Immunoelectron microscopy studies localized hCx50P88S to cytoplasmic membrane stacks in close vicinity to the endoplasmic reticulum. In contrast, aggresome-like accumulations were induced by treatment of wt hCx50-transfected cells with proteasomal inhibitors. The formation of hCx50P88S accumulations in transiently transfected cells was not blocked by treatment with Brefeldin A suggesting that they form before Cx50 transits through the Golgi apparatus to the plasma membrane. Treatment of HeLa-hCx50P88S cells with cycloheximide demonstrated the presence of a very stable pool of hCx50P88S. Taken together, these results suggest that the P to S mutation at amino acid residue 88 causes a defect that leads to decreased degradation and subsequent accumulation of hCx50P88S in a cellular structure different from aggresomes.

Keywords

Gap junction; intercellular communication; proteasome; aggresome

Introduction

Gap junctions are membrane specializations containing clusters of intercellular channels that allow intercellular passage of ions and molecules of up to 1000 Da. These channels are oligomeric assemblies of members of a family of related proteins called connexins (Cx). Six connexin monomers assemble to form a hemi-gap junction channel or connexon, which, in turn, may form a complete gap junction channel by docking with a connexon from an adjacent

1)Dr. Viviana M. Berthoud, Section of Pediatrics Hematology/Oncology, University of Chicago, 5841 S. Maryland Ave., MC 4060, Chicago, IL 60637/USA, vberthou@peds.bsd.uchicago.edu, FAX: +17737029881.

cell. Connexins are synthesized in the endoplasmic reticulum and are transported to the plasma membrane through the secretory pathway. Degradation of connexins involves the lysosomal and proteasomal pathways. The lysosomal pathway has been implicated in the degradation of gap junctions after their internalization. The proteasomal pathway has been implicated in the degradation of connexins as a quality control system for misfolded connexins and for connexins forming part of gap junctions. The half-life (or turnover rate) of most connexins as determined by pulse-chase studies is only a few hours (1.5 – 3 h) which would imply that, on average, the life-cycle of a connexin is rather short.

The lens is an avascular organ formed by an anterior epithelial cell layer and fiber cells which form the bulk of the organ. Gap junctions have been identified morphologically between epithelial cells and between fiber cells using electron microscopy (Goodenough, 1992). Their molecular components have been characterized. Lens epithelial cells express mainly Cx43 (Beyer et al., 1989; Musil et al., 1990). Mammalian lens fiber cells express Cx50 (White et al., 1992; Church et al., 1995) and Cx46 (Paul et al., 1991). Because gap junction channels allow transfer of ions and molecules of up to 1000 Da between adjacent cells, it has been proposed that they play a pivotal role for cell survival and function and, thus, for lens transparency (Goodenough, 1992). In fact, targeted disruption of the Cx50 (White et al., 1998) or Cx46 (Gong et al., 1997) gene results in cataracts in mice. Moreover, cataract-associated mutations in Cx50 (Shiels et al., 1998) or Cx46 (Mackay et al., 1999) have been identified in human families and in the No2mouse (Steele et al., 1998). The exact mechanisms for the observed phenotypes are not completely understood. However, when the proteins are expressed in *Xenopus* oocyte pairs, the human Cx46 mutants (Cx46N63S and Cx46fs380) (Pal et al., 2000) and the No 2 Cx50 mutant (Xu and Ebihara, 1999) do not induce gap junctional currents. Likewise, the missense human Cx50P88S (hCx50P88S) mutant does not induce junctional currents when expressed alone; and, when co-injected with wild-type Cx50 (wt hCx50), it impairs the ability of wt hCx50 to induce junctional currents (Pal et al., 1999).

Several steps in the life-cycle of a disease-associated connexin might be impaired. Several non-functional Cx32 mutants associated with the X-linked Charcot-Marie-Tooth disease (CMTX) have been shown not to traffic properly, to be retained in the ER or in the Golgi apparatus (Deschenes et al., 1997), and to degrade at least as rapidly as wild-type Cx32 (VanSlyke et al., 2000).

Functional studies have demonstrated that gap junction channels made of site-directed mutants of Cx26 (Suchyna et al., 1993) or Cx32 (Ri et al., 1999) in which proline 87 (corresponding to proline 88 in Cx50) was substituted with amino acids other than serine show changes in voltage gating. No further characterization of these proline-substituted connexin mutants has been reported. The present experiments were undertaken to characterize the biochemical and cellular behavior of wt hCx50 and hCx50P88S.

Materials and methods

Chemicals

All chemicals were obtained from Sigma Chemical Co. (St. Louis, MO, USA) unless otherwise specified.

Cell culture

HeLa cells were grown in DMEM supplemented with non-essential amino acids, 10% fetal bovine serum (FBS), 2 mM glutamine, 100 units/ml penicillin G and 100 μg/ml streptomycin sulfate. Neuroblastoma (N2A) cells were grown in DMEM containing high glucose, with L-glutamine and no sodium pyruvate, supplemented with 10% FBS, non-essential amino acids,

100 units/ml penicillin G and 100 μg/ml streptomycin sulfate. Normal rat kidney cells (NRK-52E, ATCC CRL 1571) were obtained from ATCC and grown in DMEM with 5% FBS, 100 units/ml penicillin G and 100 μg/ml streptomycin sulfate, non-essential amino acids and 2 mM glutamine. 293/FlpIn cells (Invitrogen, Carlsbad, CA) were grown in DMEM supplemented with 10% FBS, 2 mM glutamine, 100 units/ml penicillin G and 100 μg/ml streptomycin sulfate. Transfections were carried out using lipofectin (Invitrogen Life Technologies) or Superfect (Qiagen, Valencia, CA). Wild-type human Cx50 or hCx50P88S were subcloned into pSFFV-neo (Rup et al., 1993), and stably transfected clones were selected by their resistance to Geneticin (Invitrogen). For some tranfections, wt hCx50 or hCx50P88S were subcloned into pcDNA3.1/Hygro(+) or pcDNA5/FRT (Invitrogen), and stably transfected clones were selected by their resistance to hygromycin (Calbiochem-Novabiochem Corporation, San Diego, CA).

RNA blotting

Total cellular RNA was prepared from cell cultures using the RNeasy Mini kit (Qiagen). RNA was separated on formaldehyde/agarose gels, and transferred to Hybond N nylon membranes (Amersham, Arlington Heights, IL) as previously described (Beyer et al., 1987). Hybridization was performed using specific ^{32}P-labeled DNA probes containing the full length of the coding region of human Cx50. Probes were prepared using random hexanucleotide primers and the Klenow fragment of DNA polymerase I (Feinberg and Vogelstein, 1983).

Antibodies

Mouse monoclonal anti-protein disulphide isomerase and anti-glucose-regulated protein 94 antibodies were obtained from Affinity Bioreagents (Golden, CO). Mouse monoclonal anti-Golgi 58K protein (clone 58K-9), anti-vimentin (clone V9), anti-β-COP, and anti-β-tubulin antibodies were obtained from Sigma Chemical Company (St. Louis, MO). Mouse monoclonal anti-transferrin receptor antibodies were obtained from Zymed Laboratories, Inc. (South San Francisco, CA) and Roche Diagnostics (Indianapolis, IN). Mouse monoclonal anti-membrin antibody was obtained from Stressgen (Victoria, BC Canada). Mouse monoclonal anti-rab5 antibody was obtained from BD Transduction Laboratories (Franklin Lakes, NJ). Mouse monoclonal anti- Hsp70 antibody was obtained from Calbiochem (San Diego, CA). Mouse monoclonal anti-LAMP1 antibody developed by J. T. August and J. E. K. Hildreth was obtained from the Developmental Studies Hybridoma Bank developed under the auspices of the NICHD and maintained by The University of Iowa, Department of Biological Sciences, Iowa City, IA 52242. Cy3-conjugated goat anti-mouse IgG, FITC-conjugated goat anti-rabbit IgG, Cy2-conjugated donkey anti-rabbit IgG and HRP-conjugated goat anti-rabbit IgG antibodies were obtained from Jackson ImmunoResearch (West Grove, PA, USA). Alexa Fluor 660-conjugated goat anti-rabbit IgG was obtained from Molecular Probes (Eugene, OR).

Generation of anti-hCx50 antibodies

Apolypeptide containing an hCx50 fragment (including amino acids 231 – 433) fused to glutathione S-transferase (GST) was produced using the plasmid pGEX-3X (Amersham Biosciences, Piscataway,NJ). The purified hCx50 fusion protein was used for rabbit immunization. The rabbit serum obtained was stripped of anti-GST antibodies using a GST-immobilized agarosecolumn(Pierce, Rockford, IL).The anti-Cx50 antibodies were then affinity purified using the hCx50 fusion protein coupled to a Sulfolink column (Pierce) according to the manufacturer's directions.

Immunofluorescence

Untransfected cells or cells transfected with wt hCx50 or hCx50P88S were plated on 4-well chamber slides (LAB TEK, Nalge Nunc International, Naperville, IL, USA) and allowed to

reach 80 – 90% confluence. Cells were then rinsed with phosphate-buffered saline pH 7.4 (PBS), fixed in 4% paraformaldehyde for 15 min at room temperature, permeabilized in 1% Triton X-100 in PBS for 15 min at room temperature and blocked in 2% normal goat serum, 1% Triton X-100 in PBS for 10 min at room temperature. Cells were then incubated in mouse monoclonal antibody against proteins from different cellular compartments and/or affinity-purified rabbit polyclonal anti-Cx50 antibodies overnight at 4°C. Cells were rinsed 4 times with PBS and then incubated in secondary antibodies. After incubation at room temperature for 45 min, cells were rinsed 4 times in PBS, and coverslips were mounted with 2% n-propylgallate in PBS:glycerol (1 : 1).

Photomicrographs were obtained using a Zeiss Axioplan 2 microscope (Carl Zeiss, München, Germany) equipped with a mercury lamp and a digital camera. Measurements were performed using the Zeiss Axiovision software.

Confocal images were obtained using an IX70 Olympus Fluoview 200 laser-scanning confocal microscope (Melville,NY, USA) equipped with laser lines (488 nm, 543 nm and 633 nm). Images were collected by sequential scanning using single laser-line excitation to eliminate bleeding from one color channel into the other. Images were analyzed using Fluoview or NIH Image J software.

Electron microscopy

Thin-section electron microscopy—Hela-hCx50P88S cells were fixed overnight at room temperature with 4% glutaraldehyde (EMS, Fort Washington, PA) in 0.1 M sodium cacodylate, pH 7.3. Then, cells were washed with buffer, postfixed with 1% osmium tetroxide (EMS) for 1 hour at room temperature, washed with distilled water, and stained en bloc with 0.5% uranyl acetate at 4°C overnight. The specimens were dehydrated through a series of alcohols. Blocks were infiltrated with Epon resin:ethanol mixtures followed by 3 changes of 100% Epon resin. Blocks of cell pellets were embedded in 100% Epon, and allowed to polymerize overnight at 65°C. Ultrathin sections (70 – 90 nm) were cut on a Reichert Ultracut-E ultramicrotome (Vienna, Austria) and contrasted with uranyl acetate and lead citrate.

Immunoelectron microscopy—This procedure was performed essentially as outlined by Griffiths (1993). HeLa cells expressing hCx50P88S at 85% confluence were fixed for 15 min at room temperature in 4% paraformaldehyde (EMS), 0.5% glutaraldehyde (EMS) buffered with 0.1 M HEPES at pH 7.3. Cells were centrifuged and the fixative was replaced with fresh fixative; the cells were kept in fixative overnight at 4°C. Small pieces of the pellet were frozen on copper stubs by liquid nitrogen immersion after infiltration with 2.1 M sucrose and 0.02 M glycine in PBS. Sections (100 nm) were obtained from the cell blocks using an RMC CR-21 cryo attachment (Tucson, AZ) on a Reichert Ultracut-E ultramicrotome. Sections were blocked with 10% fetal calf serum, 0.02 M glycine in PBS for 10 min, rinsed with buffer, and incubated with rabbit anti-Cx50 antibodies (1 : 400) for one hour at room temperature. Then, sections were rinsed in PBS and incubated in 10 nm gold-conjugated protein A (Pella, Redding, CA) at a 1: 45 dilution. Sections were washed with PBS, rinsed with distilled water and stained on ice with uranyl acetate in 2% methyl cellulose (25 cps) for 10 min. All sections were collected on 200-mesh formvar-coated gold grids, and examined using a Philips CM-120 electron microscope (NewYork, NY), operated at an accelerating voltage of 120 kV. Images were collected using a CCD camera (Gatan Inc., Pleasanton, CA).

Solubility experiments

Cells at about 90% confluence were harvested in PBS supplemented with protease inhibitors and centrifuged at 150*g* for 7 min. Then, the pellets were homogenized in either 1% NP40 (10 mM Tris-HCl, pH 7.5, 5 mM EDTA, 1%NP40, 0.5% sodium deoxycholate, and 150 mM NaCl)

(Johnston et al., 1998) or RIPA buffer (50 mM Tris-HCl, pH 8.0, 1% NP40, 0.5% sodium deoxycholate, 0.1% SDS, and 150 mM NaCl) (García-Mata et al., 1999) supplemented with protease inhibitors, and then incubated for 30 min on ice. Insoluble material was recovered by centrifugation at 13 000*g* for 15 min at 4°C. The supernatant was separated from the pellet; an equal volume of Laemmli loading dye was added to the pellet. Both fractions were stored at −80°C until subjected to electrophoresis and immunoblotting.

Immunoblotting

Proteins from cell homogenates were resolved on 9% SDS-containing polyacrylamide gels, and transferred to Immobilon P membranes (Millipore, Bedford, MA). Membranes were blocked in 5% non-fat dry milk in Tris-buffered saline, pH 7.4, (TBS) for 30 min at room temperature and incubated in affinity-purified rabbit polyclonal anti- Cx50 antibodies overnight at 4°C. Then, membranes were rinsed in TBS six times, five minutes each, and incubated in HRP-conjugated goat anti-rabbit IgG antibodies for 1 h at room temperature. After this period of time, the membranes were rinsed in TBS and detection of secondary antibody binding was performed using enhanced chemiluminescence (Amersham).

Cell treatments

Brefeldin A—HeLa cells transiently or stably transfected with wt hCx50 or hCx50P88S were treated with 5, 10 or 15 μg/ml BFA or ethanol (used as a solvent for the BFA stock solution) for different lengths of time (4 and 24 h for stably transfected cells and 9 and 23 h for transiently transfected cells). Transiently transfected cells were treated with BFA 1 h after DNA transfection. Disruption of the Golgi apparatus was confirmed by immunofluorescence using a mouse monoclonal anti-Golgi 58K protein antibody.

Proteasomal inhibitors—Cells were treated with 10 μM clasto-lactacystin β-lactone (Calbiochem-Novabiochem Corporation) for 48 hours, 0.5 μM epoxomicin (Calbiochem-Novabiochem Corporation) for 24 h, or DMSO (used as a solvent for stock solutions of the proteasomal inhibitors). For some experiments, HeLa cells stably transfected with wt hCx50 were treated with both 0.5 μM epoxomicin and 5 μg/ml nocodazole for 18 or 24 h. Disruption of microtubules was confirmed by immunofluorescence using anti-β-tubulin antibodies.

Sodium 4-phenylbutyrate—HeLa-hCx50P88S cells were treated with 1 mM sodium 4-phenylbutyrate (dissolved in water) for 24 hours.

Incubation at lower temperatures—Cells were grown at 37°C until they reached 40 – 50% confluence. Then, they were either transferred to 25 °C or 30°C or left at 37 °C and further incubated until they reached 80 – 90% confluence.

Cycloheximide—Cells were treated with 40 μg/ml cycloheximide for 0, 1, 3, 12, or 21 h.

After the treatments, cells were rinsed in PBS, fixed in 4% paraformaldehyde, and processed for immunofluorescence as described above, or cells were harvested for immunoblotting after rinsing with PBS.

Labeling of endocytic pathway with fluorescent probes

Transiently transfected cells cultured in 4-well chamber slides were incubated in 1.5 mg/ml tetramethylrhodamine-conjugated dextran (MW 10000) (Molecular Probes) or 20 μg/ml Alexa Fluor 488-conjugated cholera toxin (Molecular Probes) for 7 hours; stably transfected cells were incubated in the fluorescent probes for 1 or 14 h. After that time, cells were rinsed in PBS, fixed and processed for immunofluorescence using anti-hCx50 antibodies.

Protein determination

Proteins were determined using the BioRad Protein Assay (BioRad, Hercules, CA, USA) based on the Bradford dye-binding procedure (Bradford, 1976) or by the method described by Schaffner and Weiss-man (1973).

Electrophysiology

Junctional currents between pairs of transfected cells were recorded using the double whole-cell patch-clamp technique using an Axopatch 200A amplifier (Axon Instruments, Foster City, CA) and an L/M-EPC7 amplifier (List-electronic, Germany). Patch pipettes were pulled from glass capillaries with 1.5 OD/1.0 ID (World Precision Instruments, Inc., Sarasota, FL), using a Brown-Flaming micropipette puller (Sutter Instruments, San Francisco, CA); the tips of the micropipettes were subsequently fire-polished and the resistance of the pipettes was 2 – 6 MΩ when filled with the internal pipette solution (130 mM CsCl, 10 mM EGTA, 0.5 mM $CaCl_2$, 3 mM MgATP, 2 mM Na_2ATP, 10 mM HEPES, pH 7.2). For recordings, the cell culture medium was replaced by an extracellular solution containing 140 mM NaCl, 2 mM CsCl, 2 mM $CaCl_2$, 1 mM $MgCl_2$, 5 mM HEPES, 4 mM KCl, 5 mM dextrose, 2 mM pyruvate, 1 mM $BaCl_2$, pH 7.2 (Srinivas et al., 1999; Xu et al., 2002). All experiments were performed at room temperature (22 – 24°C).

Gap junctional currents were elicited by initially holding both cells of a pair at 0 mV and applying a 5 – 10 mV pulse to one of the cells. Under these conditions, current changes recorded in the second cell would be equal in magnitude and opposite in polarity to the current flowing through gap junction channels. Gap junctional conductance, g_j, was calculated as the ratio of the change in current recorded in the second cell divided by the applied difference in voltage. Data are presented as the mean ± standard error of the mean.

Results

Stable transfection of wild-type human connexin50 and human connexin50P88S - Determination of function

We have previously shown that expression of hCx50P88S in *Xenopus* oocytes results in no junctional currents (Pal et al., 1999). This could result from improper trafficking/targeting, formation of non-functional channels, and/or other alterations in the life-cycle of the connexin. Because the *Xenopus* oocyte system is not ideal to elucidate potentially altered steps in the connexin life-cycle, we transfected mammalian cell lines with wt hCx50 or hCx50P88S.

Stably transfected clones of N2A, HeLa, NRK, and 293 cells were analyzed for their expression of wt hCx50 and hCx50P88S by RNA blot hybridization. A band of the expected size was detected in the transfected clones (shown for HeLa cells in Fig. 6G). The presence of Cx50 protein was assessed by immunoblotting (Fig. 1); a band of $M_r \approx 62$ kDa was detected in the transfected clones. This band had an electrophoretic mobility indistinguishable from the Cx50 band detected in human lens homogenates, and it was absent in homogenates from untransfected cells.

The formation of functional gap junction channels was analyzed using the double whole-cell patch-clamp technique. The junctional conductance between pairs of cells transfected with either wt hCx50 or hCx50P88S was determined from the current obtained when applying 5 – 10 mV transjunctional voltages (Table I). Wild-type hCx50 formed functional channels in N2A cells and in HeLa cells. The junctional conductance of cells expressing wt hCx50 was significantly higher than that determined in untransfected cells from either cell line. In contrast, N2A cells transfected with the mutant, hCx50P88S, showed no detectable junctional

conductance; HeLa cells transfected with the hCx50P88S showed significantly lower junctional conductance than either untransfected cells or cells transfected with wt hCx50.

Previous experiments have also shown that hCx50P88S decreases the magnitude of the wt hCx50-induced gap junctional currents in the *Xenopus* oocyte expression system (Pal et al., 1999). To test whether hCx50P88S behaved similarly in mammalian cells, wt hCx50-expressing N2A cells were transfected with hCx50P88S, and stable clones were obtained using a different selectable marker (hygromycin). The expression of both wt hCx50 and hCx50P88S in N2A cells was assessed by hybridization of RNA blots with a Cx50 probe. Because cells had been transfected with wt hCx50 in pSFFV-neo vector and hCx50P88S in pcDNA3.1/Hygro (+) vector, it was expected that the mRNAs derived from these two constructs would be of different size. Total RNA prepared from N2A cells transfected with wt hCx50 showed one band while co-transfected cells showed two: one corresponding to the wild-type Cx50 mRNA and the other corresponding to the mutant Cx50 mRNA (Fig. 2). The co-expressing cells were analyzed for the presence of functional channels by the double whole-cell patch-clamp technique. No junctional conductance was detected in any of the cell pairs analyzed from two different clones of N2A co-transfectants (Table I).

Distribution of anti-Cx50 immunoreactivity in transfected cells

The distribution of Cx50 in stable transfectants was assessed by immunofluorescence (Fig. 3). Cells transfected with wt hCx50 showed staining at appositional membranes and in the cytoplasm as expected for transfected connexins (Fig. 3A, C, F). In contrast, cells transfected with hCx50P88S showed intense staining in cytoplasmic accumulations of immunoreactivity to anti-Cx50 antibodies (Fig. 3B, D, G, H). Generally, one to five accumulations were found at different locations in the cytoplasm of each cell; measurements of inclusions in HeLa cells showed that their diameters ranged from 0.6 to 2.7 μm. The prominence of the staining at appositional membranes varied between different cell types transfected with hCx50P88S; plasma membrane staining was very infrequent in N2A cells, occasional in HeLa cells and commonly observed in NRK cells (Fig. 3). N2A cells co-transfected with wt hCx50 and hCx50P88S showed cytoplasmic accumulations of Cx50 immunoreactivity and staining at appositional membranes (Fig. 3E).

Studies in transfected cells have shown that several mutant Cx32 proteins associated with CMTX are retained in the ER or in the Golgi compartment, and they do not localize at appositional membranes (Deschenes et al., 1997; VanSlyke et al., 2000). To assess whether the hCx50P88S accumulations were present in the ER or Golgi, or whether they were associated with another specific subcellular compartment, we performed double-label immunofluorescence in HeLa-hCx50P88S cells using antibodies directed against resident proteins of the ER (GRP94 and PDI), Golgi (β-COP, membrin and 58K protein), lysosomes (LAMP1), endocytic pathway (transferrin receptor, rab5), or stress-related chaperones (Hsp70) and anti-Cx50 antibodies. No significant co-localization was observed between any of these compartment-specific proteins and the cytoplasmic accumulations of immunoreactive Cx50 (Fig. 4A – D). (Occasional co-localization of membrin or rab5 immunoreactivity with small spots of Cx50 immunoreactivity was observed.) Moreover, no co-localization of Cx50 immunoreactivity with tetramethylrhodamine-conjugated dextran or Alexa Fluor 488-conjugated cholera toxin (used as markers of endosomes/rafts) was observed in HeLa cells either stably or transiently transfected with hCx50P88S (Fig. 4E, F).

Because connexins are plasma membrane proteins, they would be expected to be transported along the secretory pathway from their place of synthesis in the rough endoplasmic reticulum to the Golgi and from there to the plasma membrane. To test whether wt hCx50 was delivered to the plasma membrane through the secretory pathway, the distribution of Cx50 was analyzed by immunofluorescence after treatment of HeLa-wt hCx50 cells with BFA (a drug that disrupts

the Golgi and protein trafficking to the plasma membrane). This treatment disrupted the Golgi apparatus as assessed by the dispersion of the immunoreactivity to the anti-Golgi 58K protein antibody (compare Fig. 5A and B, red channel). The distribution of Cx50 immunoreactivity was drastically changed after treatment with BFA (compare Fig. 5A and B, green channel). Several Cx50-immunoreactive spots were observed intracellularly after treatment with BFA; most of the Cx50 immunoreactivity detected at appositional membranes under control conditions (Fig. 5A, green channel) was absent in cells treated with BFA (Fig. 5B, green channel); in very rare occasions some Cx50 immunoreactivity was observed at the plasma membrane.

Once we had proven that hCx50 is delivered to the plasma membrane through the secretory pathway, it was of interest to test whether hCx50P88S accumulations formed in an early secretory compartment. HeLa cells stably transfected with hCx50P88S were treated with BFA for up to 24 hours, and the distribution of the mutant protein was assessed by immunofluorescence. The Cx50 inclusions observed in HeLa cells stably transfected with hCx50P88S were unaffected by BFA treatment (not shown). In transiently transfected cells, Cx50 immunoreactivity was first detected 6 h post-transfection. Eight hours after transfection, immunoreactivity localized to very small round structures. Larger immunoreactive inclusions were observed at 24 h. Treatment with BFA 1 h after transfection did not affect the formation of accumulations of Cx50 immunoreactivity. These accumulations were similar in size and shape to those observed in untreated cells (Fig. 5C, D).

Degradation of mutant Cx50

Mutations in proteins may also alter their degradation. To test whether the degradation of hCx50 was altered due to the presence of the P88S missense mutation, cells transfected with either wt hCx50 or hCx50P88S were treated with 40 μg/ml cycloheximide for 0 – 21 h, and the homogenates were analyzed after immunoblotting. Levels of Cx50 decreased during the first few hours of cycloheximide treatment in both wt hCx50- and hCx50P88S-transfected HeLa cells; however, after a longer duration of cycloheximide treatment, levels of Cx50 were much lower in wt hCx50-transfected cells than in hCx50P88S-transfected cells (Fig. 6A, B). In agreement with these results, cycloheximide-treated HeLa-wt hCx50 cells showed a general decrease in Cx50-immunofluorescent staining with persistence of some diffuse and small particulate cytoplasmic staining and some appositional membrane staining; in contrast, cycloheximide-treated hCx50P88S-transfected cells showed persistence of the large accumulations with some decrease in small Cx50-immunoreactive accumulations (Fig. 6C – F). Northern blot analysis of untreated HeLa-wt hCx50 and HeLa-hCx50P88S cells showed very similar levels of mRNA expression (Fig. 6G). However, the levels of Cx50 protein in immunoblots were higher in cells transfected with the mutant connexin than in cells transfected with the wild-type protein (Fig. 6H); when normalized to vimentin levels (Fig. 6I), the Cx50 levels in HeLa-hCx50P88S were 1.7-fold as great as those of cells transfected with wild-type connexin.

Are these Cx50P88S accumulations aggresomes?

Several mutant proteins, including a mutant of CFTR, accumulate in cellular structures called aggresomes (Johnston et al., 1998; García-Mata et al., 1999; Kabore et al., 2001; Waelter et al., 2001). Aggresomes have been proposed to be generated in response to an overload of misfolded proteins which are normally degraded by the proteasome (Kopito, 2000; Garcia-Mata et al., 2002). They would form by coalescence of small accumulations of proteins that travel along microtubules towards the microtubule organizing center. Characterization of aggresomes in other systems has shown that these inclusions are usually surrounded by a cage of vimentin. To assess whether the hCx50P88S accumulations met this criteria, we performed double immunofluorescence using anti-vimentin and anti-Cx50 antibodies. These experiments

showed little correlation between vimentin and Cx50 staining (Fig. 7A). Moreover, when samples were analyzed by confocal microscopy, the vimentin and Cx50 stainings were detected in different focal planes of the optical section (Fig. 7B). After reconstruction of a z-series of confocal sections, many of the Cx50 accumulations resembled doughnut- or C-shaped structures.

Formation of aggresomes in other systems has been induced by treatment of cells with proteasomal inhibitors (García-Mata et al., 1999; Waelter et al., 2001). To test whether the wild-type Cx50 could form aggresomes (and whether they resembled the accumulations observed in hCx50P88S-transfected cells), HeLa cells transfected with wt hCx50 were treated with clasto-lactacystin-β-lactone or epoxomicin. When treated HeLa-wt hCx50 cells were analyzed by immunofluorescence, a significant proportion of Cx50 immunoreactivity collapsed into a single large area (Fig. 8, compare panels A and B) that appeared more compact after treatment with epoxomicin. Similarly, the filamentous staining observed with anti-vimentin antibodies in untreated cells (Fig. 8C) collapsed after treatment with proteasomal inhibitors (Fig. 8D). A high degree of co-localization between the two signals was observed in proteasomal inhibitor-treated cells (Fig. 8, compare panels E and F). Treatment of cells with proteasomal inhibitors in the presence of nocodazole blocked the collapse of the Cx50 immunoreactivity observed in cells treated with proteasomal inhibitors only. In contrast, when HeLa-hCx50P88S cells were treated with epoxomicin or clasto-lactacystin-β-lactone, the accumulations of Cx50 immunoreactivity remained unaltered; minimal, if any, co-localization with vimentin was observed (not shown).

Characterization of aggresomes in other systems has also shown that these accumulations are highly insoluble in various detergents (Johnston et al., 1998; García-Mata et al., 1999).The solubility properties of transfected wt hCx50 or hCx50P88S proteins were assessed using 1% NP40 or RIPA buffer. In untreated cells, virtually all Cx50 immunoreactivity was detected in the 13 000*g* pellet of either wt hCx50 or hCx50P88S-transfected cells (Fig. 9, lanes 1 and 2). At least 90% of immunoreactive Cx50 was solubilized by RIPA buffer for both wild-type and mutant hCx50 (Fig. 9, lanes 5 and 6). However, when treated with 1% NP40, more than 85% of the wild-type protein was detected in the supernatant, but only about 40% of the mutant protein was soluble in this detergent (Fig. 9, lanes 3 and 4).

To test whether proteasomal inhibitor-induced Cx50 accumulations had similar solubility properties to aggresomes, the detergent solubility of these Cx50 accumulations was investigated. In epoxomicin-treated HeLa-wt hCx50 cells, the 1% NP40 or RIPA buffer supernatant contained substantially decreased Cx50 immunoreactivity (50 – 60%) as compared to untreated cells (Fig. 9A, lanes 9 – 12).To test whether inhibition of the proteasome altered the solubility of the mutant Cx50, HeLa cells transfected with hCx50P88S were also treated with epoxomicin. Under these conditions, the solubility of hCx50P88S in 1% NP40 was not significantly altered by proteasomal inhibitor treatment, but the RIPA buffer supernatant contained substantially decreased Cx50 immunoreactivity (50 – 60%) as compared to untreated cells (Fig. 9B, lanes 9 – 12).

Electron microscopy studies

To identify the subcellular compartment/structure(s) in which the transfected connexin was localized, we performed electron microscopy studies on HeLa-hCx50P88S cells. When thin-section electron microscopy was performed, vesicles with single membranes were frequently seen, and these vesicles were larger and more numerous in cells expressing mutant protein. In addition, circular or semicircular membrane stacks were identified within the cytoplasm of cells. These structures had a similar size and location to the doughnut and C-shaped structures seen by immunofluorescence (Fig. 10A). In most instances, these membrane stacks appeared to be individual sheets in close apposition similar to the appearance of normal gap junctions

(Fig. 10A, arrowheads). However, the ends of some of these stacks separated to form clear lumenal spaces (Fig. 10A, arrow). These individual membranes curved around to make contact with other membranes about 5 – 10 stacks away (Fig. 10A, asterisk). When membranes curved in the cell, they often moved out of the plane of section, which made it difficult to determine the exact localization of these membrane curves. Nevertheless, the overall series of multilayered membrane structures was not surrounded by an individual membrane sheet. Rough ER membranes (as judged by punctate dots along membrane contiguous with the nuclear membrane) were observed close to both the nuclear and the cytoplasmic sides of the stacks (Fig. 10). These structures were not observed in cells transfected with wt hCx50.

Examination of these cells using cryo-immunoelectron microscopy revealed many small vesicles that were moderately positive for anti-Cx50 immunoreactivity, each surrounded by a single membrane. The presence of very closely apposed membrane stacks intensely labeled with anti-Cx50 antibodies was sometimes observed in these preparations (Fig. 10B); in most instances, the gold particles were located on the outside of each membrane (Fig. 10C).Gold particles were also seen in the cytoplasm surrounded by the stacks of membrane and close to the plasma membrane. No gold particles were observed in multivesicular bodies (Fig. 10D) or in the nuclear envelope.

Distribution of anti-Cx50 immunoreactivity after incubation of cell cultures at reduced temperatures or after treatment with a chemical chaperone

Folding/trafficking defects in several membrane protein mutants have been overcome by chemical chaperones or by decreasing the temperature at which cells are incubated (Denning et al., 1992; Rubenstein et al., 1997). To test for possible folding/trafficking defects of hCx50P88S expressed in HeLa or N2A cells, HeLa-hCx50P88S or N2A-hCx50P88S were shifted from incubation at 37 °C to 25°C or 30°C, and the distribution of Cx50 was assessed by immunofluorescence (Fig. 11). Cells shifted to temperatures lower than 37°C showed increased anti-Cx50 immunoreactivity at appositional membranes as compared to cells that remained at 37°C (Fig. 11, compare panels A and D to panels B and E, respectively). Similarly, treatment of HeLa-hCx50P88S with sodium 4-phenylbutyrate led to an increase in Cx50 immunoreactivity at appositional membranes (Fig. 11C); a decrease in the size of the cytoplasmic Cx50 accumulations was also apparent after this treatment (Fig. 11C). However, growth at reduced temperatures did not restore proper function, since double whole-cell patch-clamp analysis of N2A-hCx50P88S cells did not show any increase in junctional conductance (not shown).

Discussion

The results presented in this paper have shown a striking difference between the distribution of wild-type hCx50 and hCx50P88S. Wild-type protein localizes to the plasma membrane, but hCx50P88S localizes in cytoplasmic inclusions. The distribution of wt hCx50 in the cytoplasm and at appositional membranes is consistent with its appropriate targeting and assembly into gap junctions as reported for other transfected wild-type connexins (Eghbali et al., 1990; Steinberg et al., 1994; Traub et al., 1994). Cells transfected with wild-type and mutant Cx50 also differed in Cx50 protein levels; higher levels of Cx50 were detected in hCx50P88S-transfected cells. This difference did not result from increased RNA expression as mRNA levels were similar; rather, from a reduced degradation rate of the mutant protein, since after treatment with cycloheximide a very stable pool of Cx50 immunoreactivity was detected only in cells expressing the mutant protein.

The results presented in this study have also shown that while transfection of mammalian cells with wt hCx50 induced junctional conductance, transfection of hCx50P88S into N2A cells produced no junctional conductance. Moreover, introduction of hCx50P88S significantly

decreased (or abolished) the junctional conductance detected in HeLa cells or in wt hCx50-expressing N2A cells. These results extend our previous observations in *Xenopus* oocytes (Pal et al., 1999) by suggesting that hCx50P88S is unable to induce junctional currents when expressed by itself in mammalian cells and that it can inhibit not only wt hCx50-induced junctional conductance but also the endogenous gap junctional conductance present in HeLa cells (possibly due to Cx45). The presence of some Cx50 immunoreactivity at the plasma membrane in hCx50P88S-transfected cells suggests that the mutant Cx50 formed non functional channels. Moreover, because some mutant protein reached the plasma membrane, the functional data obtained in cells co-transfected with wild-type and mutant Cx50 argue that hCx50P88S acted as a dominant negative inhibitor of the wild-type hCx50.

Several connexin mutants associated with human diseases have been reported in recent years. The cellular mechanisms leading to the disease phenotype may differ among connexin mutants. Studies of CMTX-associated Cx32 mutants have revealed that while some Cx32 mutants reach the plasma membrane, several non-functional mutants are retained in the endoplasmic reticulum or in the Golgi apparatus (Deschenes et al., 1997; VanSlyke et al., 2000). In the present study, a significant proportion of the non-functional mutant, hCx50P88S, was observed in cytoplasmic accumulations. The lack of significant co-localization of hCx50P88S accumulations with resident proteins of the endoplasmic reticulum or Golgi apparatus suggests that the mutant protein was not retained in either of these compartments. Moreover, while the CMTX-associated Cx32 mutants are degraded at least as fast as the wild-type protein (VanSlyke et al., 2000), hCx50P88S-transfected HeLa cells contained a very stable pool of Cx50 protein. Thus, the data suggest that the P88S missense mutation in hCx50 induced a distinct defect, not previously reported for a connexin.

Several mutant proteins (including CFTR) accumulate in the cytoplasm in structures that have been named aggresomes (Johnston et al., 1998; García-Mata et al., 1999; Kabore et al., 2001; Waelter et al., 2001). The current hypothesis is that aggresomes originate as a consequence of exceeding the degradative capacity of the proteasome; small protein aggregates dispersed throughout the cell travel along microtubules towards the microtubule organizing center where they coalesce to form aggresomes. These accumulations are characterized by their detergent insolubility and, in most cases, by being surrounded by a cage of vimentin. Treatment of wt hCx50-transfected HeLa cells with proteasomal inhibitors induced the collapse of Cx50 immunoreactivity into an area where it co-localized with vimentin immunoreactivity through a process that was dependent on microtubule integrity; this effect was also associated with an increase in insolubility of Cx50- immunoreactive material. Overall, these results suggest that wt hCx50 can form aggresome-like accumulations when the degradative capacity of the proteasome is exceeded; they also imply that, similar to Cx43 (Laing and Beyer, 1995), the proteasomal pathway participates in the degradation of wt hCx50. In contrast, the hCx50P88S cytoplasmic accumulations did not co-localize with vimentin. While aggresomes are insoluble in RIPA buffer, hCx50P88S was highly soluble. Treatment with proteasomal inhibitors did not alter the distribution or appearance of hCx50P88S accumulations. The differences in the results obtained in proteasomal inhibitor-treated wt hCx50-transfectants and untreated hCx50P88S-transfected cells argue that the hCx50P88S accumulations observed in this study do not correspond to aggresomes; at the same time, they argue that the hCx50P88S accumulations are formed at a step in the life-cycle of the connexin different than that affected by the proteasomal inhibitors in wt hCx50-transfected cells.

Degradation of connexins can occur through the lysosomal or the proteasomal pathway. Gap junctional plaques appear to be degraded by lysosomes after internalization by endocytosis. The lack of co-localization of hCx50P88S with markers of the endosome/lysosome compartment or of immunogold labeling in multivesicular bodies suggest that hCx50P88S did not accumulate within components of this compartment. Cytoplasmic connexins can be

degraded by the proteasome; this process may occur after dislocation of connexins from the ER (by ER-associated degradation, ERAD), which in the case of Cx43 appears to be regulated by cytosolic stress (Van Slyke and Musil, 2002). The altered degradation of hCx50P88S observed in the present study apparently resulted from trapping of the mutant protein in a compartment in which it could not undergo normal degradation. The electron microscopy data suggest that this compartment contained stacks of double membranes. Gold particles were observed on the outside of each membrane within a stack indicating that hCx50P88S was inserted into the membrane in the correct topological orientation (since the antibody was raised to a fusion protein containing the carboxyl terminus of hCx50). These stacks of double membrane are different from the multilamellar bodies described by Gilliland et al. (2001), but are reminiscent of the “internal gap junctions” observed in BHK cells transfected with Cx32 under the control of an inducible promoter (Kumar et al., 1995). Based on the presence of gap junctions in the nuclear envelope and its continuity with the ER, Kumar et al. (1995) concluded that the membrane stacks originated from the ER. The formation of hCx50P88S accumulations in transiently transfected cells in the presence of BFA, a drug that disrupts the Golgi apparatus, suggests that these inclusions form from an early secretory compartment, most likely the ER or ERGIC. Zampighi et al. (1999) have reported that reflexive gap junctions can form in single *Xenopus* oocytes expressing Cx50 when the expressed connexin attains a threshold of hemichannel density/membrane unit area. Thus, it is possible that hCx50P88S cannot be degraded in this membrane compartment and reaches a threshold concentration triggering the formation of the observed accumulations.

Several lines of evidence suggest that hCx50P88S can be targeted to the plasma membrane under some conditions. First, a significant amount of Cx50 immunoreactivity was observed at appositional membranes in transfected NRK cells. Second, the proportion of hCx50P88S immunoreactivity at appositional membranes in N2A or HeLa cells could be increased after either a temperature shift or treatment with sodium 4-phenylbutyrate. These conditions have been used to overcome defects in cell surface localization and function for some disease-associated mutant proteins leading to the suggestion that these mutants have folding/trafficking defects (Denning et al., 1992; Rubenstein et al., 1997). Thus, the results obtained in this study suggest that hCx50P88S has some folding/trafficking defect that becomes evident when expressed in N2A or HeLa cells. Because of the presence of some hCx50P88S immunoreactivity at the plasma membrane and the structure of the membrane stacks observed by transmission electron microscopy, most likely it is a defect in trafficking. The different proportions of hCx50P88S present at membrane appositions in N2A, HeLa and NRK cells might reflect the presence in NRK cells of a more efficient system that facilitates folding/trafficking of the mutant protein and/or a higher expression of adhesion molecules and increased appositional membrane area. A relation between expression of adhesion molecules and formation of gap junctional plaques has been previously reported (Musil et al., 1990; Jongen et al., 1991; Meyer et al., 1992). Alternatively, because NRK cells express Cx43 and it has been reported that wild-type Cx43 or Cx43-EGFP can rescue a Cx43-DsRed chimera that is retained in intracellular compartments (Lauf et al., 2001), it is possible that the endogenous Cx43 in NRK cells rescues the trafficking defect of hCx50P88S. This interpretation would imply that wild-type Cx43 could interact with and facilitate trafficking of the mutant hCx50; and, at the same time it would imply that the interaction between these connexins occurs in an early compartment of the secretory pathway. However, the increase in Cx50 at appositional membranes observed when N2A-hCx50P88S cells were grown at reduced temperatures was not accompanied by restoration of function as no junctional conductance was detected by double whole-cell patch-clamp.

The hypothesis that gap junctional intercellular communication is crucial for lens transparency has been substantiated by the gene ablation studies in mice (Gong et al., 1997; White et al., 1998) and the identification of human (Shiels et al., 1998; Mackay et al., 1999) and mouse

(Steele et al., 1998) cataract-associated connexin mutants. In the mammalian lens, Cx50 is highly expressed in fiber cells. Because hCx50P88S-containing channels are not functional, the presence of this mutant in the lens could induce cataract formation by decreasing intercellular communication between lens cells. Any loss-of-function connexin mutant would thus be expected to cause a similar cataract due to the generalized decrease in gap junctional intercellular communication. Whether accumulations of hCx50P88S also occur in the lenses of affected individuals is not known. However, the presence of multilamellar bodies with diameters of 1 – 3 μm in cataractous lenses has led Gilliland et al. (2001) to propose these bodies as possible light scattering particles. If the accumulations of hCx50P88S (which had similar diameters) also formed in lens cells, they might likewise interfere with lens transparency and thus contribute to the zonular pulverulent cataracts observed in affected individuals.

In summary, our observations suggest that the P to S mutation at position 88 in connexin50 causes a trafficking defect that can be rescued by incubation at lower temperatures or by co-expression with wild-type Cx43. The proportion of the protein that is unable to continue along its normal pathway for incorporation into gap junction plaques or to dislocate for ERAD likely accumulates in a cytoplasmic membrane compartment leading to the formation of inclusions that are different from aggresomes.

Abbreviations

BFA, Brefeldin A
CFTR, Cystic fibrosis transmembrane regulator
CMTX, X-linked Charcot-Marie-Tooth disease
Cx, Connexin
ERAD, ER-associated degradation
GST, Glutathione S-transferase
hCx50P88S, Human Cx50 containing a proline to serine mutation at amino acid residue 88
LAMP1, Lysosome-associated membrane protein 1
N2A, Neuro2A mouse neuroblastoma cell line
RIPA, buffer 50 mM Tris-HCl, pH 8.0, 1% NP40, 0.5% sodium deoxycholate, 0.1% SDS, and 150 mM NaCl
wt hCx50, Wild-type human Cx50

Acknowledgements

The authors greatly appreciate the helpful comments of Dr. Agustín Martínez and the technical assistance of Naga Aithal and Emily Christensen. These studies were funded by NIH grants EY08368 and HL59199 (to E. C. Beyer) and EY10589 (to L. Ebihara).

References

Beyer EC, Paul DL, Goodenough DA. Connexin43: a protein from rat heart homologous to a gap junction protein from liver. J. Cell Biol 1987;105:2621–2629. [PubMed: 2826492]

Beyer EC, Kistler J, Paul DL, Goodenough DA. Antisera directed against connexin43 peptides react with a 43-kD protein localized to gap junctions in myocardium and other tissues. J. Cell Biol 1989;108:595–605. [PubMed: 2537319]

Bradford MM. A rapid and sensitive method for the quantitation of microgram quantities of protein using the principle of protein-dye binding. Anal. Biochem 1976;72:248–254. [PubMed: 942051]

Church RL, Wang JH, Steele E. The human lens intrinsic membrane protein MP70 (Cx50) gene – clonal analysis and chromosome mapping. Curr. Eye Res 1995;14:215–221. [PubMed: 7796604]

Denning GM, Anderson MP, Amara JF, Marshall J, Smith AE, Welsh MJ. Processing of mutant cystic fibrosis transmembrane conductance regulator is temperature sensitive. Nature 1992;358:761–764. [PubMed: 1380673]

Deschenes SM, Walcott JL, Wexler TL, Scherer SS, Fischbeck KH. Altered trafficking of mutant connexin32. J. Neurosci 1997;17:9077–9084. [PubMed: 9364054]

Eghbali B, Kessler JA, Spray DC. Expression of gap junction channels in communication-incompetent cells after stable transfection with cDNA encoding connexin 32. Proc. Natl. Acad. Sci. USA 1990;87:1328–1331. [PubMed: 2154741]

Feinberg AP, Vogelstein B. A technique for radiolabelling DNA restriction endonuclease fragments to high specific activity. Anal. Biochem 1983;132:6–13. [PubMed: 6312838]

García-Mata R, Bebok Z, Sorscher EJ, Sztul ES. Characterization and dynamics of aggresome formation by a cytosolic GFP-chimera. J. Cell Biol 1999;146:1239–1254. [PubMed: 10491388]

García-Mata R, Gao Y-S, Sztul E. Hassles with taking out the garbage: aggravating aggresomes. Traffic 2002;3:388–396. [PubMed: 12010457]

Gilliland KO, Freel CD, Lane CW, Fowler WC, Costello MJ. Multilamellar bodies as potential scattering particles in human age-related nuclear cataracts. Mol. Vis. 2000 2001;7:120–130.

Gong X, Li E, Klier G, Huang Q, Wu Y, Lei H, Kumar NM, Horwitz J, Gilula NB. Disruption of α3 connexin gene leads to proteolysis and cataractogenesis in mice. Cell 1997;91:833–843. [PubMed: 9413992]

Goodenough DA. The crystalline lens. A system networked by gap junctional intercellular communication. Semin. Cell Biol 1992;3:49–58. [PubMed: 1320431]

Griffiths, G. Fine structure immunocytochemistry. Heidelberg, Germany: Springer-Verlag; 1993.

Johnston JA, Ward CL, Kopito RR. Aggresomes: A cellular response to misfolded proteins. J. Cell Biol 1998;143:1883–1898. [PubMed: 9864362]

Jongen WM, Fitzgerald DJ, Asamoto M, Piccoli C, Slaga TJ, Gros D, Takeichi M, Yamasaki H. Regulation of connexin 43-mediated gap junctional intercellular communication by Ca^{2+} in mouse epidermal cells is controlled by E-cadherin. J. Cell Biol 1991;114:545–555. [PubMed: 1650371]

Kabore AF, Wang WJ, Russo SJ, Beers MF. Biosynthesis of surfactant protein C: characterization of aggresome formation by EGFP chimeras containing propeptide mutants lacking conserved cysteine residues. J. Cell Sci 2001;114:293–302. [PubMed: 11148131]

Kopito RR. Aggresomes, inclusion bodies and protein aggregation. Trends Cell Biol 2000;10:524–530. [PubMed: 11121744]

Kumar NM, Friend DS, Gilula NB. Synthesis and assembly of human β1 gap junctions in BHK cells by DNA transfection with the human β1 cDNA. J. Cell Sci 1995;108:3725–3734. [PubMed: 8719879]

Laing JG, Beyer EC. The gap junction protein connexin43 is degraded via the ubiquitin proteasome pathway. J. Biol. Chem 1995;270:26399–26403. [PubMed: 7592854]

Lauf U, Lopez P, Falk MM. Expression of fluorescently tagged connexins: a novel approach to rescue function of oligomeric DsRed-tagged proteins. FEBS Lett 2001;498:11–15. [PubMed: 11389889]

Mackay D, Ionides A, Kibar Z, Rouleau G, Berry V, Moore A, Shiels A, Bhattacharya S. Connexin46 mutations in auto-somal dominant congenital cataract. Am. J. Hum. Genet 1999;64:1357–1364. [PubMed: 10205266]

Meyer RA, Laird DW, Revel JP, Johnson RG. Inhibition of gap junction and adherens junction assembly by connexin and A-CAM antibodies. J. Cell Biol 1992;119:179–189. [PubMed: 1326565]

Musil LS, Beyer EC, Goodenough DA. Expression of the gap junction protein connexin43 in embryonic chick lens: molecular cloning, ultrastructural localization, and post-translational phosphorylation. J. Membr. Biol 1990;116:163–175. [PubMed: 2166164]

Musil LS, Cunningham BA, Edelman GM, Goodenough DA. Differential phosphorylation of the gap junction protein connexin43 in junctional communication-competent and -deficient cell lines. J. Cell Biol 1990;111:2077–2088. [PubMed: 2172261]

Pal JD, Berthoud VM, Beyer EC, Mackay D, Shiels A, Ebihara L. Molecular mechanism underlying a Cx50-linked congenital cataract. Am. J. Physiol 1999;276:C1443–C1446. [PubMed: 10362609]

Pal JD, Liu X, Mackay D, Shiels A, Berthoud VM, Beyer EC, Ebihara L. Connexin46 mutations linked to congenital cataract show loss of gap junction channel function. Am. J. Physiol 2000;279:C596–C602.

Paul DL, Ebihara L, Takemoto LJ, Swenson KI, Goodenough DA. Connexin46, a novel lens gap junction protein, induces voltage-gated currents in nonjunctional plasma membrane of *Xenopus* oocytes. J. Cell Biol 1991;115:1077–1089. [PubMed: 1659572]

Ri Y, Ballesteros JA, Abrams CK, Oh S, Verselis VK, Weinstein H, Bargiello TA. The role of a conserved proline residue in mediating conformational changes associated with voltage gating of Cx32 gap junctions. Biophys. J 1999;76:2887–2898. [PubMed: 10354417]

Rubenstein RC, Egan ME, Zeitlin PL. In vitro pharmacologic restoration of CFTR-mediated chloride transport with sodium 4-phenylbutyrate in cystic fibrosis epithelial cells containing ÄF508-CFTR. J. Clin. Invest 1997;100:2457–2465. [PubMed: 9366560]

Rup DM, Veenstra RD, Wang HZ, Brink PR, Beyer EC. Chick connexin56, a novel lens gap junction protein. J. Biol. Chem 1993;268:706–712. [PubMed: 7678009]

Schaffner W, Weissman C. A rapid, sensitive, and specific method for the determination of protein in dilute solution. Anal. Biochem 1973;56:502–514. [PubMed: 4128882]

Shiels A, Mackay D, Ionides A, Berry V, Moore A, Bhattacharya S. A missense mutation in the human connexin50 gene (GJA8) underlies autosomal dominant “zonular pulverulent” cataract, on chromosome 1q. Am. J. Hum. Genet 1998;62:526–532. [PubMed: 9497259]

Srinivas M, Costa M, Gao Y, Fort A, Fishman GI, Spray DC. Voltage dependence of macroscopic and unitary currents of gap junction channels formed by mouse connexin50 expressed in rat neuroblastoma cells. J. Physiol. (Lond) 1999;517:673–689. [PubMed: 10358109]

Steele EC Jr, Lyon MF, Favor J, Guillot PV, Boyd Y, Church RL. A mutation in the connexin 50 (Cx50) gene is a candidate for the No 2 mouse cataract. Curr. Eye Res 1998;17:883–889. [PubMed: 9746435]

Steinberg TH, Civitelli R, Geist ST, Robertson AJ, Hick E, Veenstra RD, Wang HZ, Warlow PM, Westphale EM, Laing JG, Beyer EC. Connexin43 and connexin45 form gap junctions with different molecular permeabilities in osteoblastic cells. EMBO J 1994;13:744–750. [PubMed: 8112289]

Suchyna TM, Xu LX, Gao F, Fourtner CR, Nicholson BJ. Identification of a proline residue as a transduction element involved in voltage gating of gap junctions. Nature 1993;365:847–849. [PubMed: 8413670]

Traub O, Eckert R, Lichtenberg-Frate H, Elfgang C, Bastide B, Scheidtmann KH, Hülser DF, Willecke K. Immunochemical and electrophysiological characterization of murine connexin40 and -43 in mouse tissue and transfected human cells. Eur. J. Cell Biol 1994;64:101–112. [PubMed: 7957300]

VanSlyke JK, Deschenes SM, Musil LS. Intracellular transport, assembly, and degradation of wild-type and disease-linked mutant gap junction proteins. Mol. Biol. Cell 2000;11:1933–1946. [PubMed: 10848620]

VanSlyke JK, Musil LS. Dislocation and degradation from the ER are regulated by cytosolic stress. J. Cell Biol 2002;157:381–394. [PubMed: 11980915]

Waelter S, Boeddrich A, Lurz R, Scherzinger E, Lueder G, Lehrach H, Wanker EE. Accumulation of mutant huntingtin fragments in aggresome-like inclusion bodies as a result of insufficient protein degradation. Mol. Biol. Cell 2001;12:1393–1407. [PubMed: 11359930]

White TW, Bruzzone R, Goodenough DA, Paul DL. Mouse Cx50, a functional member of the connexin family of gap junction proteins, is the lens fiber protein MP70. Mol. Biol. Cell 1992;3:711–720. [PubMed: 1325220]

White TW, Goodenough DA, Paul DL. Targeted ablation of connexin50 in mice results in microphthalmia and zonular pulverulent cataracts. J. Cell Biol 1998;143:815–825. [PubMed: 9813099]

Xu X, Ebihara L. Characterization of a mouse Cx50 mutation associated with the No 2 mouse cataract. Invest. Ophthalmol. Vis. Sci 1999;40:1844–1850. [PubMed: 10393059]

Xu X, Berthoud VM, Beyer EC, Ebihara L. Functional role of the carboxyl terminal domain of human connexin50 in gap junctional channels. J. Membr. Biol 2002;186:101–112. [PubMed: 11944087]

Zampighi GA, Loo DDF, Kreman M, Eskandari S, Wright EM. Functional and morphological correlates of connexin50 expressed in *Xenopus laevis* oocytes. J. Gen. Physiol 1999;113:507–523. [PubMed: 10102933]

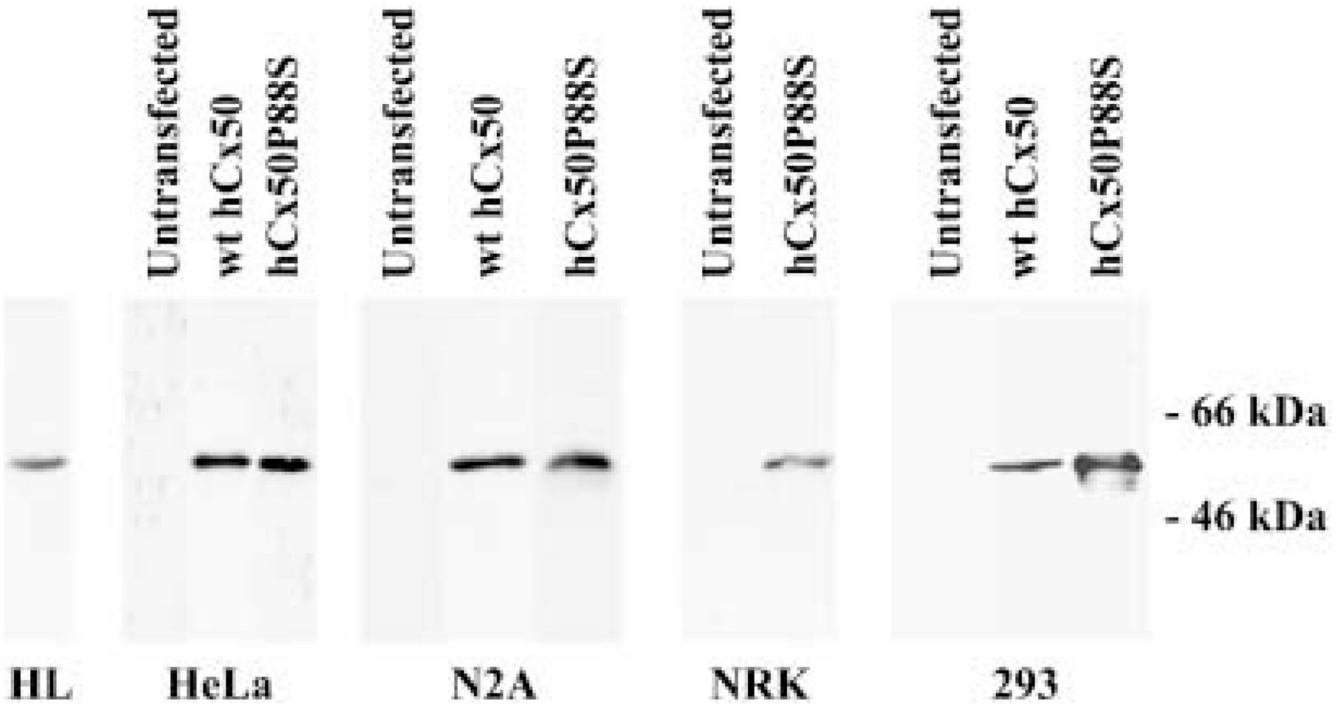

Fig. 1.

Detection of wild-type human Cx50 or Cx50P88S protein in transfected cells. Proteins from whole cell homogenates of untransfected N2A, HeLa, NRK or 293 cells or cells transfected with wt hCx50 or hCx50P88S were resolved by SDS-PAGE and subjected to immunoblotting using rabbit polyclonal anti-human Cx50 antibodies. A sample from a human lens homogenate (HL) was used as a positive control. The positions of the 66- and 46-kDa molecular mass standards are indicated on the right.

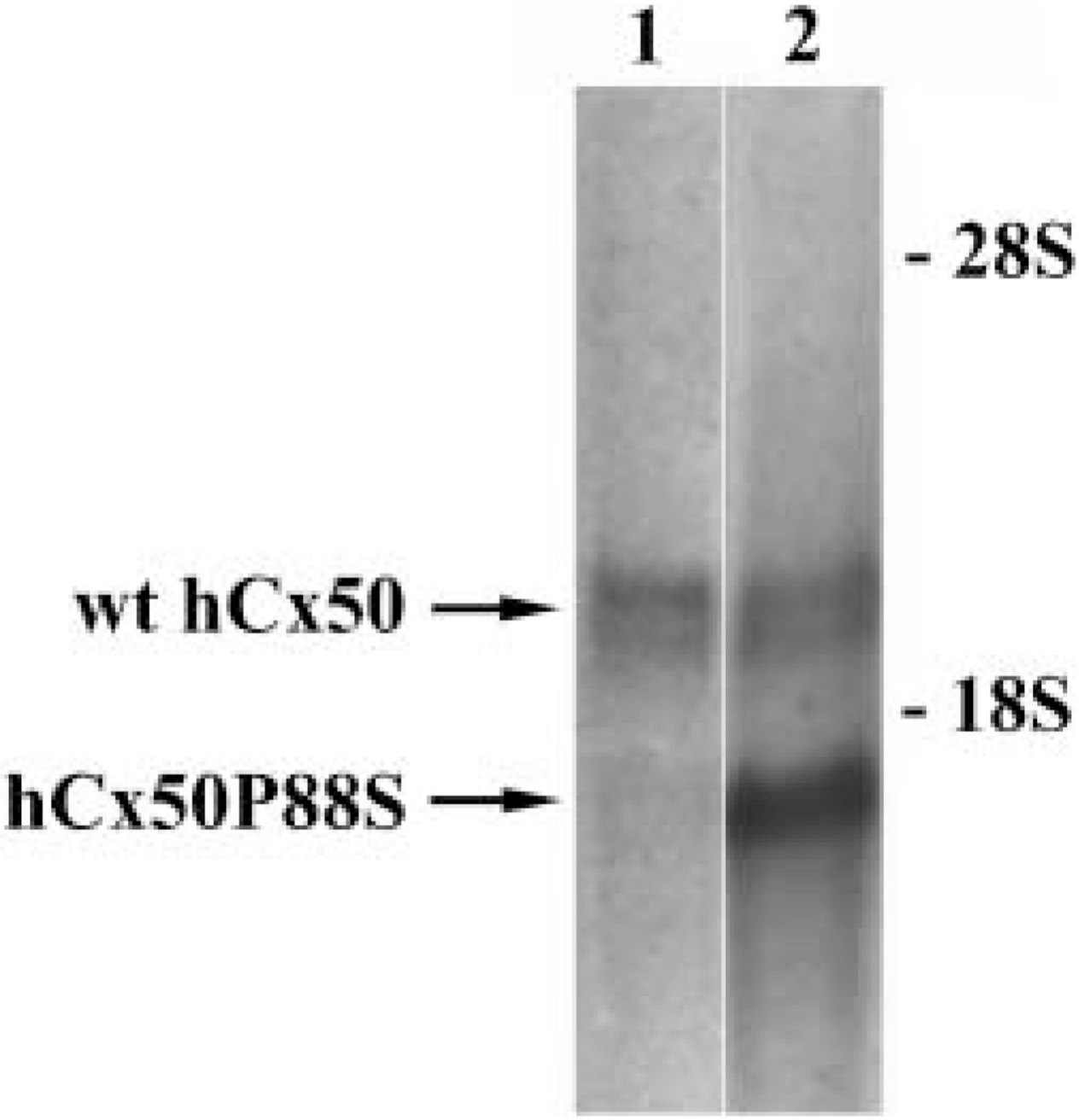

Fig. 2.

Co-expression of wild-type hCx50 and hCx50P88S. Total RNA from N2A cells transfected with wild-type hCx50 (*lane 1*) or both human wild-type hCx50 and hCx50P88S (*lane 2*) was hybridized with a hCx50 probe. The identities of the hybridizing bands are indicated by *arrows*. Because cells were transfected with wt hCx50 in the pSFFV-neo vector and hCx50P88S in the pcDNA3.1/Hygro(+) vector, the sizes of the mRNAs differ. The positions of the 18S and 28S ribosomal RNAs are indicated.

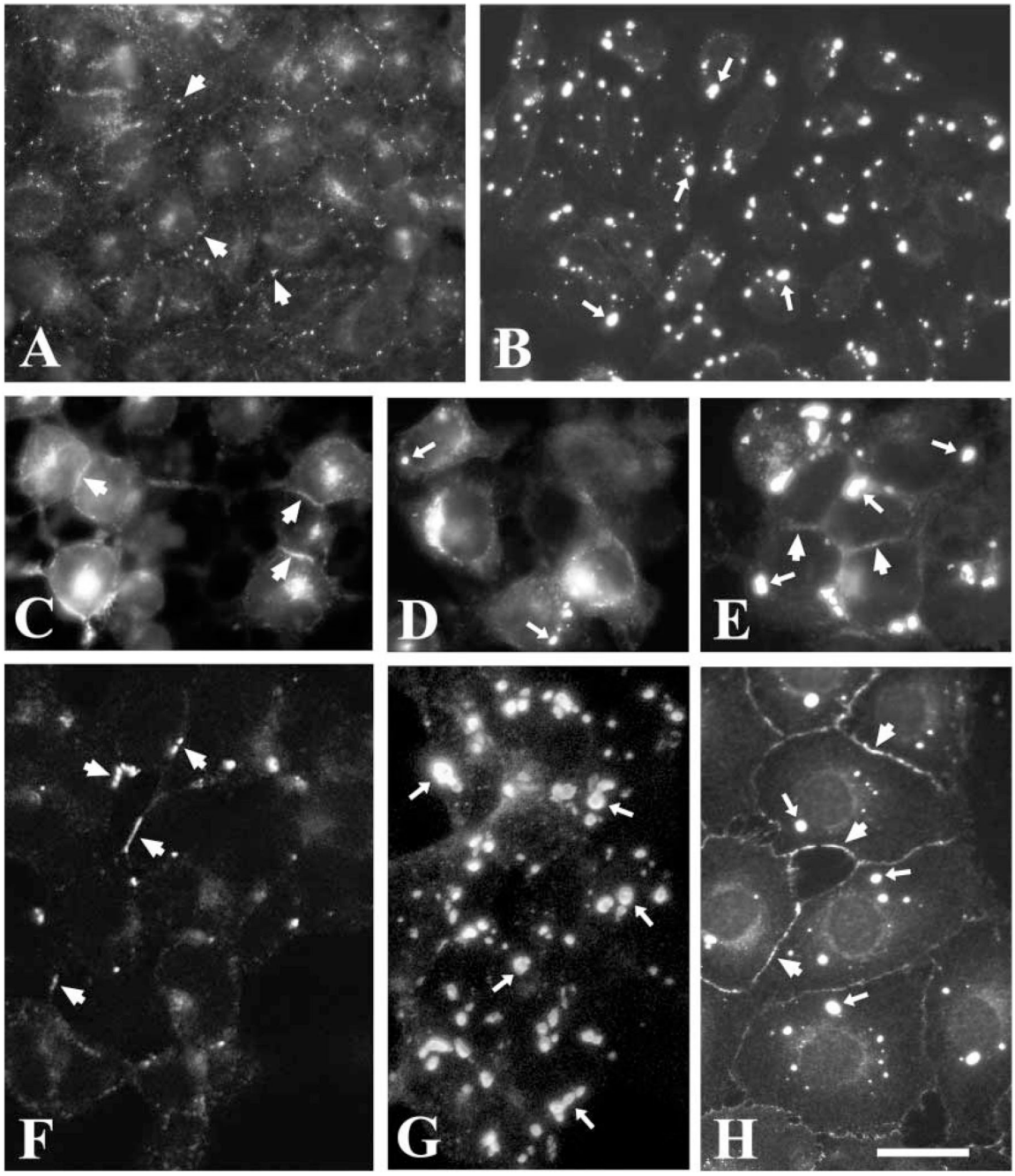

Fig. 3.

Distribution of anti-Cx50 immunoreactivity in transfected cells. Photomicrographs show the distribution of anti-Cx50 immunoreactivity in HeLa (**A, B**), N2A (**C, D, E**), 293 (**F, G**) and NRK (**H**) cells transfected with human wild-type Cx50 (**A, C, F**), hCx50P88S (**B, D, G, H**), or both wild-type and mutant hCx50 (**E**). Panel **F** is a confocal image and panel **G** is a reconstruction of a confocal z series. Staining at membrane appositions (*short arrows*) and cytoplasmic accumulations (*long arrows*) is indicated. Bar represents 35 μm in **A**, 37 μm in **B**, 21 μm in **C** and **D**, 31 μm in **E, F** and **G**, and 33 μm in **H**.

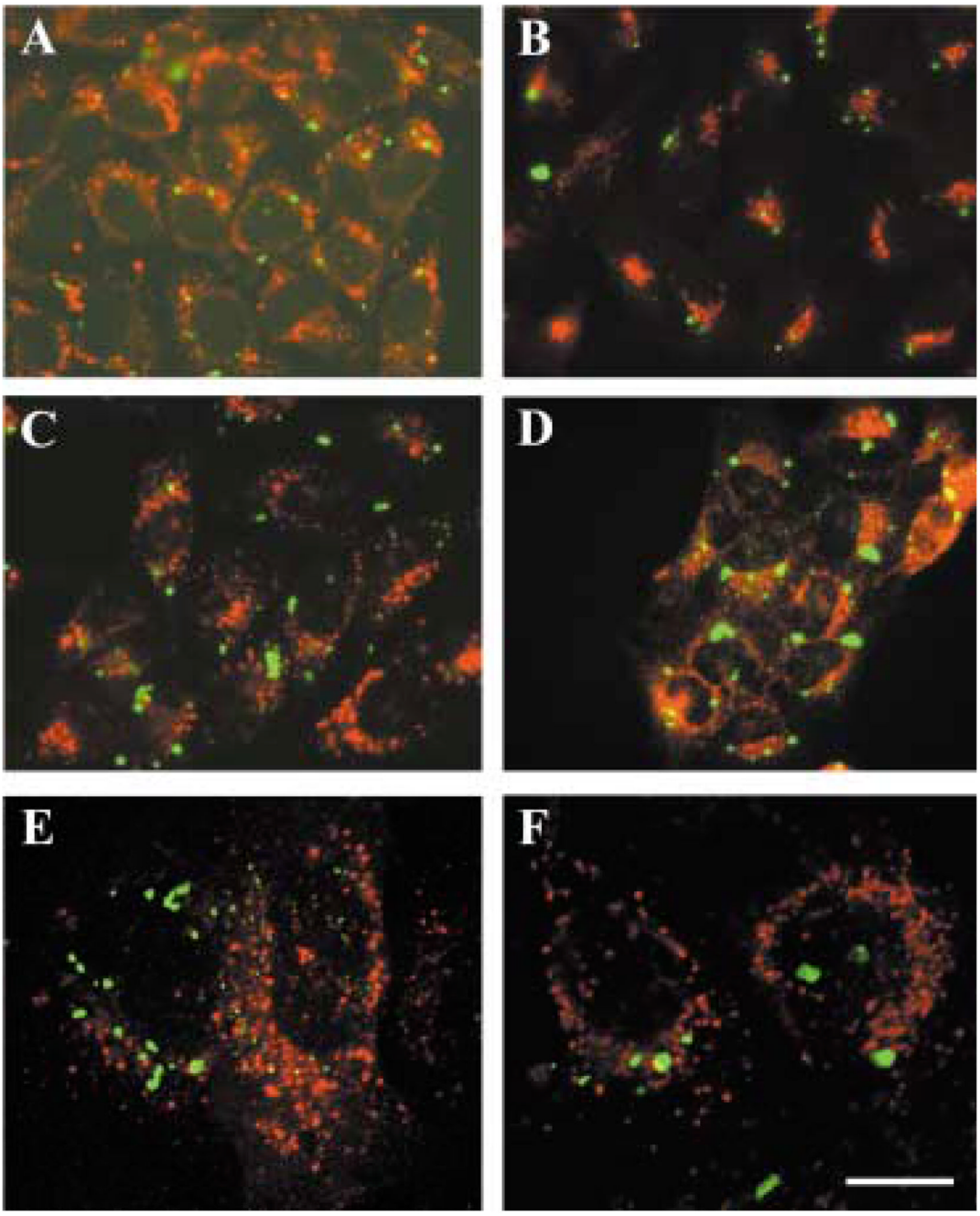

Fig. 4.

Lack of co-localization of anti-Cx50 immunoreactivity with several cellular compartments. (**A–D**) Photomicrographs of double-immunofluorescence staining of HeLa cells stably transfected with hCx50P88S using rabbit polyclonal anti-Cx50 antibodies and a mouse monoclonal antibody directed against (**A**) protein disulfide isomerase (an endoplasmicretic reticulum-resident protein), (**B**) Golgi 58K protein (a Golgi-resident protein), (**C**) the lysosome-associated membrane protein 1 (LAMP1), or (**D**) transferrin receptor (a marker for the endocytic pathway). (**E, F**) Photomicrographs of HeLa cells transiently (**E**) or stably (**F**) transfected with hCx50P88S showing the lack of co-localization of Cx50 immunoreactivity with tetramethylrhodamine-dextran (shown in *red*) used as a different marker for the endocytic

pathway. Anti-Cx50 immunoreactivity is shown in *green*; immunoreactivity to the antibodies against proteins from specific cellular compartments is shown in *red*. Bar represents 31 μm in **A**, 27 μm in **B** and **C**, 47 μm in **D**, 14 μm in **E** and 12 μm in **F**.

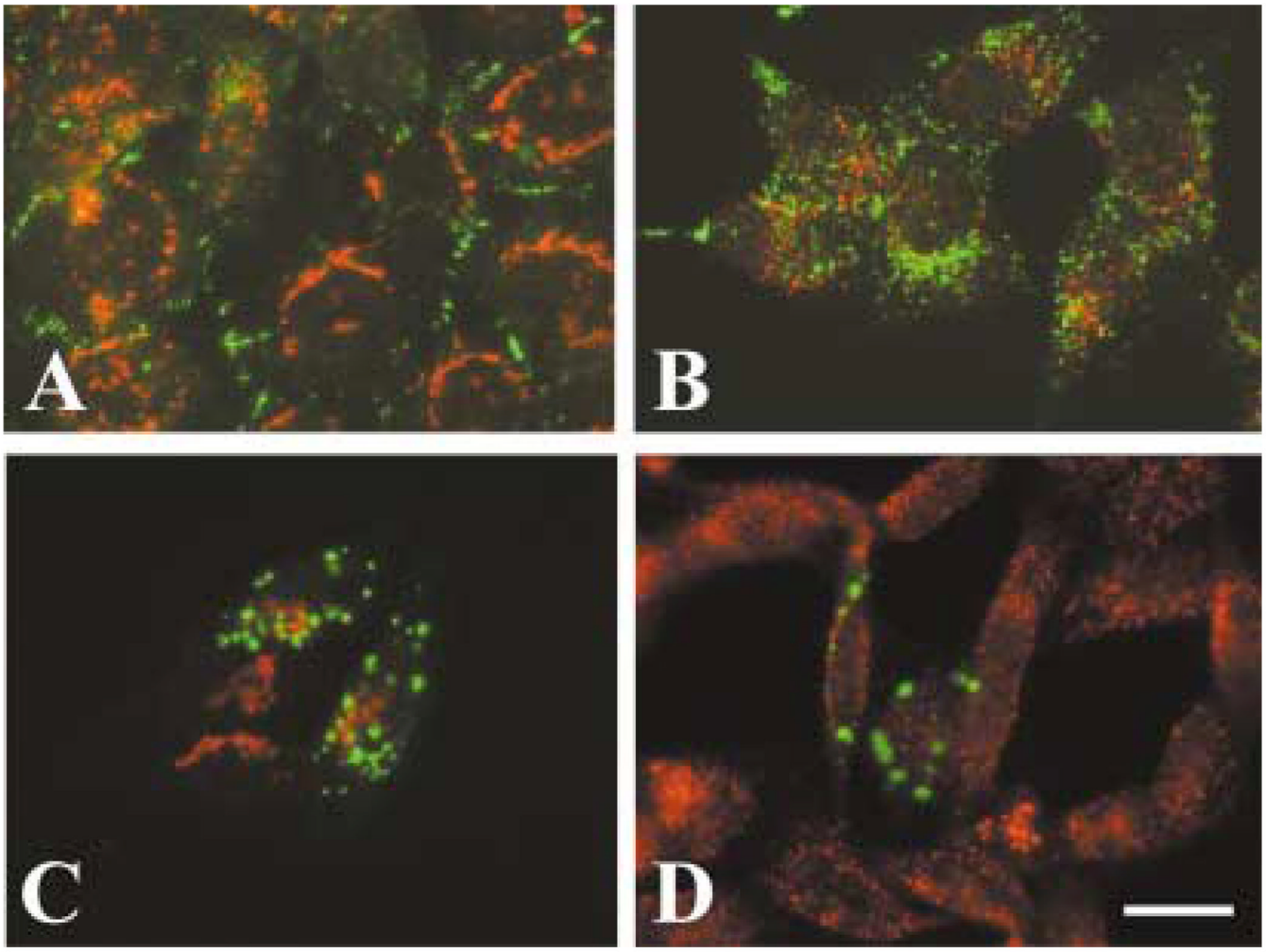

Fig. 5.

Accumulations of hCx50P88S form before the protein transits through the Golgi to the plasma membrane. Photomicrographs showing the distribution of Cx50 (*green*) and Golgi 58K protein (*red*) immunoreactivities in HeLa cells stably transfected with wt hCx50 (**A, B**) or transiently transfected with hCx50P88S (**C, D**) under control conditions (**A, C**) or after treatment with BFA (**B, D**). For the transient transfection experiments, BFA treatment started 1 h after DNA transfection; cells were fixed 24 h after transfection and then processed for immunofluorescence. Co-localization of the two signals appears *yellow*. Bar represents 21 μm.

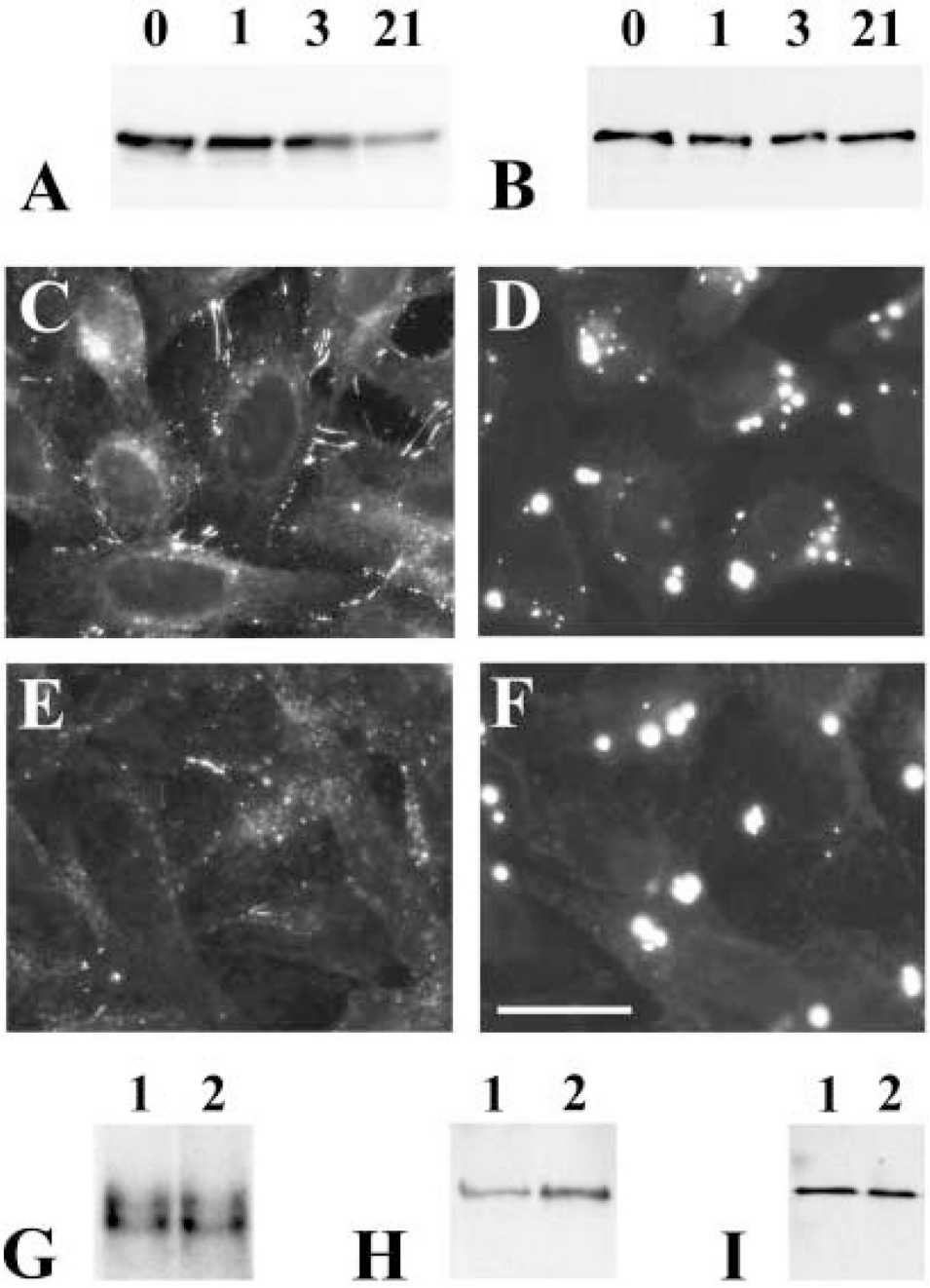

Fig. 6.

Presence of a stable pool of immunoreactive Cx50 in cells transfected with hCx50P88S. (**A, B**) Immunoblots of homogenates from HeLa-wt hCx50 (**A**) or HeLa-hCx50P88S (**B**) cells that were left untreated (*lanes 0*) or treated with 40 μg/ml cycloheximide for 1, 3 or 21 h (*lanes 1, 3, 21*, respectively) using anti-Cx50 antibodies. (Exposure times for **A** and **B** were different). (**C–F**) Photomicrographs showing Cx50 immunoreactivity in HeLa cells transfected with wild-type hCx50 (**C, E**) or hCx50P88S (**D, F**) that were left untreated (**C, D**) or treated with cycloheximide for 12 hours (**E, F**). (**G**) Northern blot of Cx50 RNA from HeLa-wt hCx50 (*lane 1*) and HeLa-hCx50P88S (*lane 2*) cells hybridized with a hCx50 probe. (Because cells were transfected with DNAs encoding wt hCx50 or hCx50P88S in the same vector, pSFFV-

neo, the mRNA sizes of wt hCx50 and hCx50P88S are identical). (**H, I**) Immunoblots of homogenates from HeLa-wt hCx50 (*lanes 1*) and HeLa-hCx50P88S (*lanes 2*) cells reacted with anti-Cx50 (**H**) or antivimentin (**I**) antibodies. Bar represents 29 μm in **C**, and 26 μm in **D, E** and **F**.

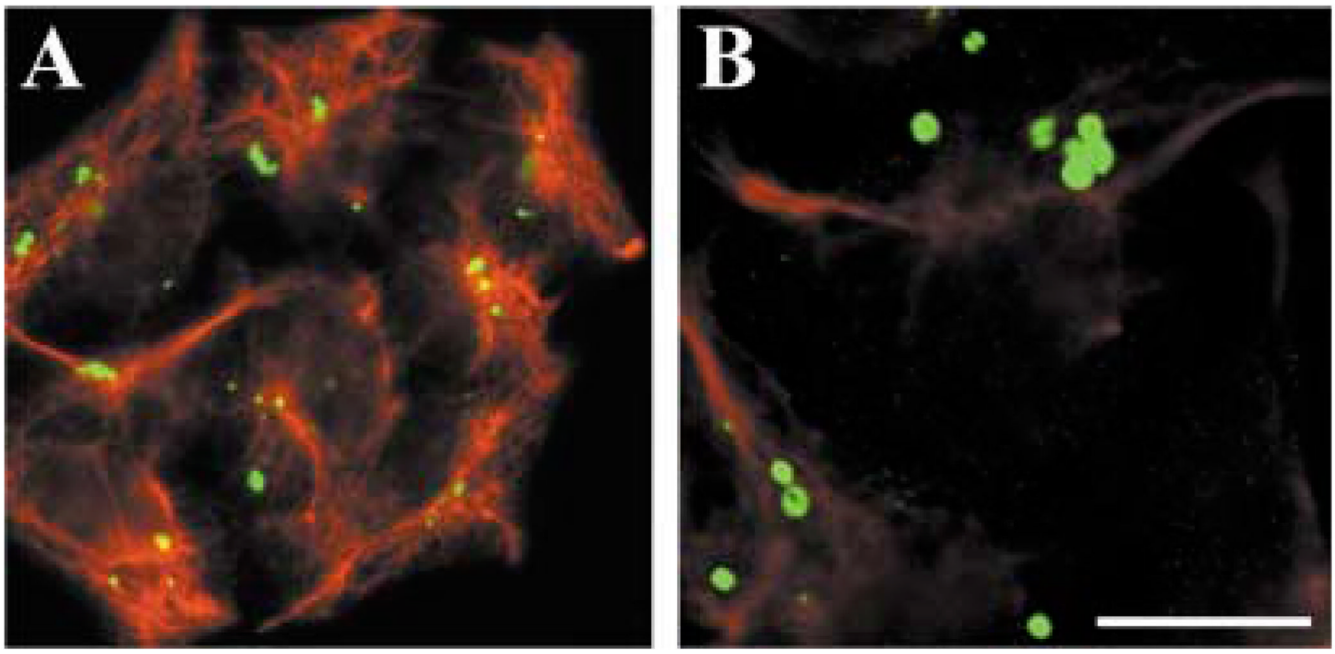

Fig. 7.

Absence of co-localization of hCx50P88S accumulations with vimentin. Anti-Cx50 (*green*) and anti-vimentin (*red*) immunoreactivities after double-immunofluorescence staining of HeLa cells transfected with hCx50P88S. An epifluorescence photomicrograph is shown in **A**; a confocal image is shown in **B**. Bar represents 33 μm in **A** and 13 μm in **B**.

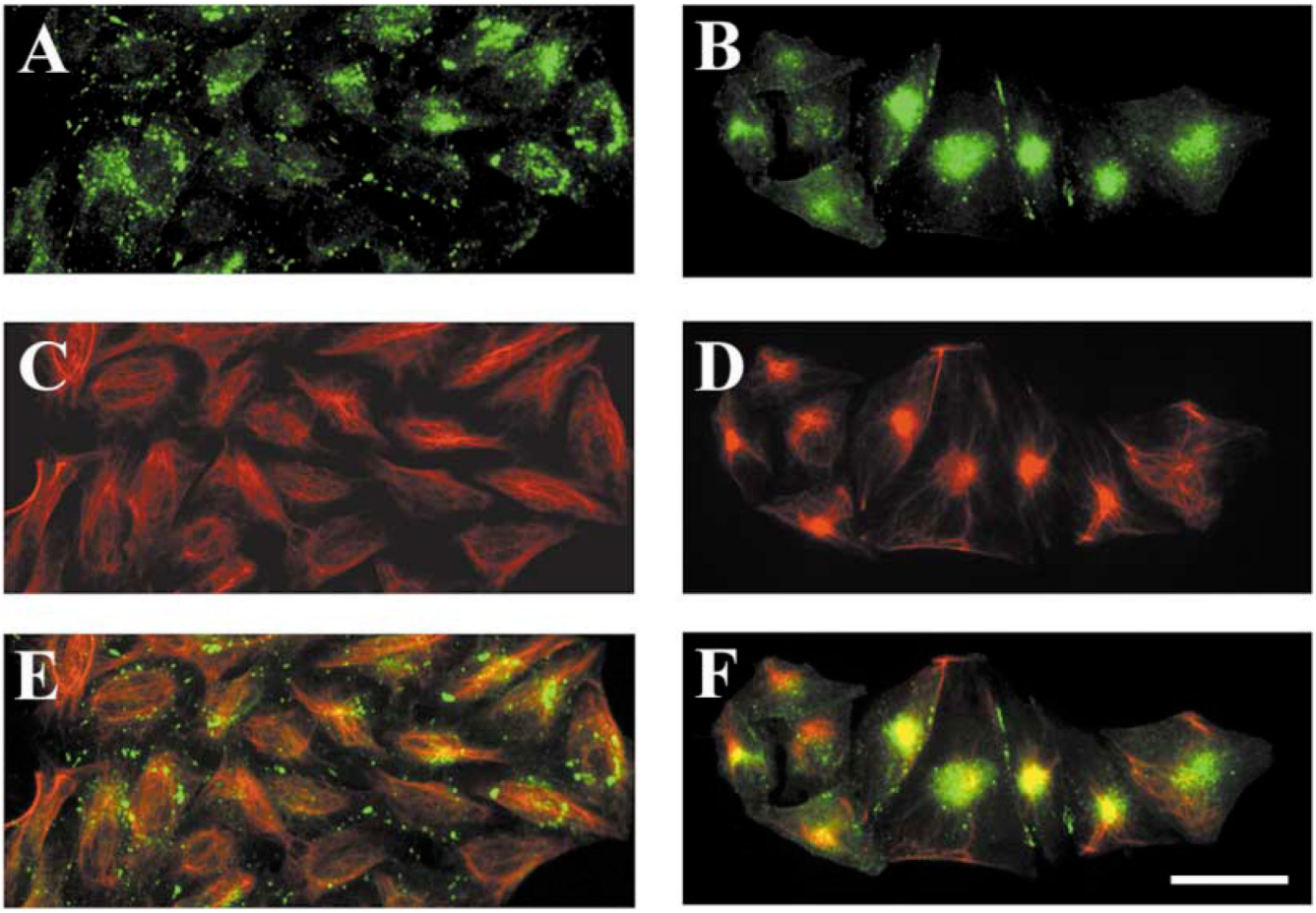

Fig. 8.

Induction of accumulations of wt hCx50 following treatment of cultured cells with proteasomal inhibitors. Photomicrographs of HeLa cells transfected with wt hCx50 cultured under control conditions (**A, C, E**) or treated with 10 μM clasto-lactacystin β-lactone (**B, D, F**) after double-label immunostaining using anti-Cx50 (*green*; **A, B**) and anti-vimentin (*red*; **C, D**) antibodies. Superposition of the two signals is shown in **E** and **F**; the overlap between the two signals appears *yellow*. Bar represents 46 μm.

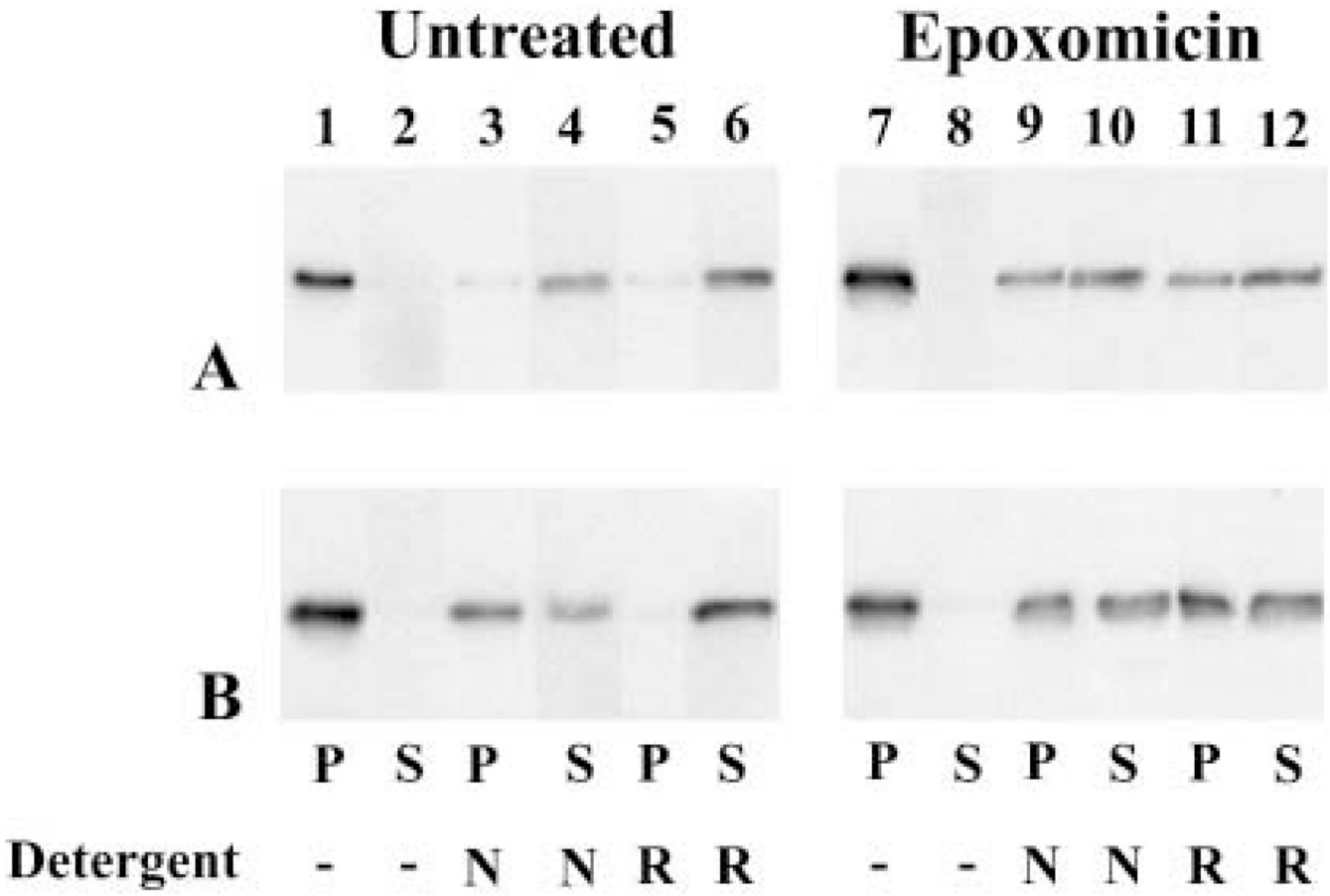

Fig. 9.

Solubility of Cx50 in HeLa cells and effects of proteasomal inhibitor treatment. Homogenates prepared from HeLa cells transfected with wt hCx50 (**A**) or hCx50P88S (**B**) under control conditions (*lanes 1 – 6*) or after treatment with 0.5 μM epoxomicin (*lanes 7 – 12*) were incubated in the absence or in the presence of 1% NP40 (N) or RIPA buffer (R). After 30 min, the samples were centrifuged at 13 000*g* and the pellets (P) were separated from the supernatants (S) and subjected to immunoblotting.

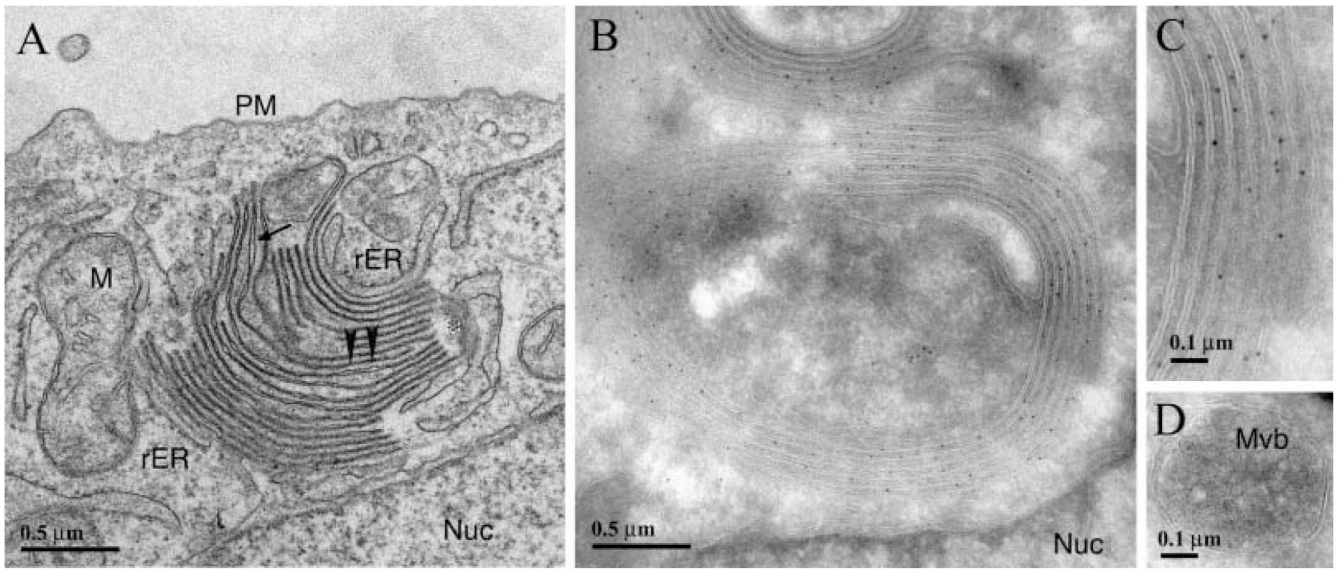

Fig. 10.

Electron micrographs showing the fine structure and immunogold labeling of HeLa-hCx50P88S cells. (**A**) Transmission electron micrograph showing the presence of membrane stacks in the cytoplasm of these cells; in most areas, membranes are closely apposed (*arrowheads*) similar to the appearance of normal gap junctions, but other regions of the membrane show a widened intermembrane space (*arrow*). Rough ER (rER) is seen associated with membrane stacks. These individual membranes curve around to make contact with other membranes about 5 – 10 stacks away (*). (**B** and **C**) Cryosections of immunogold stained specimens showing membrane stacks. Membrane stacks showed intense labeling with anti-Cx50 antibodies; these labeled rings of membranes correspond to those identified by transmission electron microscopy (different orientation of profile). An enlarged view is shown in **C**. (**D**) Cryo-immunolocalization was used to examine classic multi-vesicular bodies (Mvb) in these cells. In no case, were any Mvbs seen to react with anti-Cx50 antibodies.

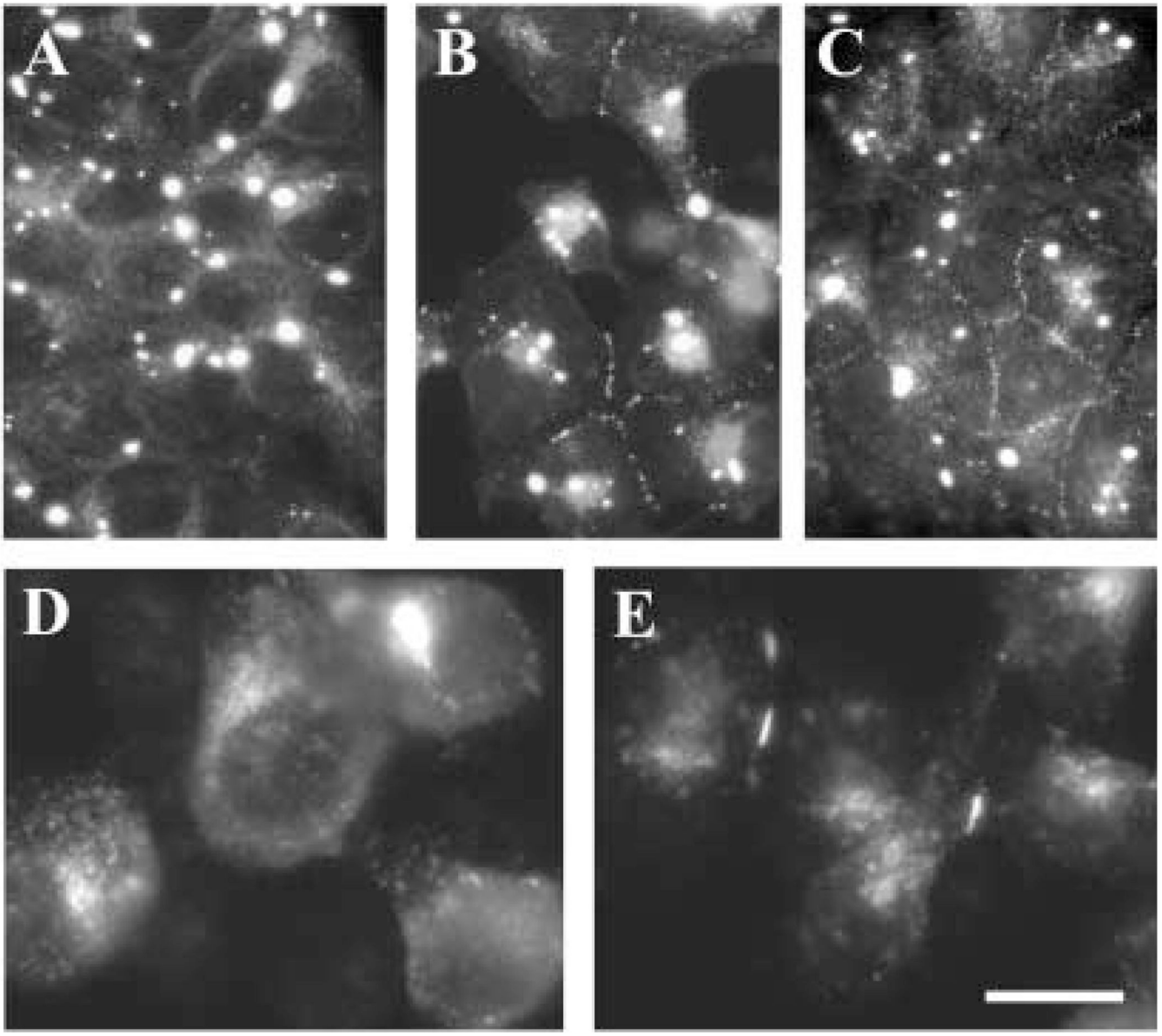

Fig. 11.

Increased hCx50P88S immunoreactivity at appositional membranes after incubation at lower temperatures or in the presence of chemical chaperones. Photomicrographs of anti-Cx50 immunoreactivity from HeLa (**A–C**) or N2A (**D, E**) cells transfected with hCx50P88S grown at 37 °C and kept at 37 °C (**A, C, D**) or shifted to 30°C (**E**) or 25°C (**B**) grown under control conditions (**A, B, D, E**) or treated with 1 mM sodium 4-phenylbutyrate for 24 hours (**C**). Bar represents 50 μm in **A**, 62 μm in **B**, 31 μm in **C**, and 13 μm in **D** and **E**.

Tab. I

Junctional conductances observed in cells expressing wt hCx50 or hCx50P88S

Cell line	Transfected connexin (clone #)	G_j (nS) Mean ± SEM	n
N2A	None	0.04 ± 0.38[a]	56
	wt hCx50 (8)	2.81 ± 0.38	95
	wt hCx50 (18)	1.78 ± 0.47	48
	hCx50P88S (4)	0.00 ± 0.00[a]	30
	hCx50P88S (12)	0.00 ± 0.00[a]	30
	wt hCx50 + hCx50P88S (8)	0.00 ± 0.00[a]	35
	wt hCx50 + hCx50P88S (12)	0.00 ± 0.00[a]	36
HeLa	None	2.8 ± 0.6	110
	wt hCx50	13.4 ± 1.6[b]	40
	hCx50P88S	1.1 ± 0.5[b]	68

Junctional conductance of pairs of N2A or HeLa cells transfected with wt hCx50, hCx50P88S or both was measured by the dual whole-cell patch-clamp technique. Values represent the mean ± standard error of the mean (SEM); n = number of cell pairs.

[a] $p<0.05$(Student×s t-test compared to N2A-wt hCx50);

[b] $p<0.05$(Student×s t-test compared to untransfected HeLa cells). The data from N2A cells transfected with wt hCx50 have been reported by Xu et al. (2002).